Published in final edited form as:
Exp Cell Res. 2014 February 15; 321(2): 123–132. doi:10.1016/j.yexcr.2013.12.003.

Alpha-2 Heremans Schmid Glycoprotein (AHSG) Modulates Signaling Pathways in Head and Neck Squamous Cell Carcinoma Cell Line SQ20B

Pamela D. Thompson[a], **Amos Sakwe**[a], **Rainelli Koumangoye**[b], **Wendell G. Yarbrough**[c], **Josiah Ochieng**[a], and **Dana R. Marshall**[d,*]

[a]Department of Biochemistry and Cancer Biology, Meharry Medical College, Nashville, TN 37208, USA

[b]Division of Surgical Oncology and Endocrine Surgery, Vanderbilt University Medical Center, Nashville, TN 37232, USA

[c]Division of Otolaryngology, Departments of Surgery and Pathology and Yale Cancer Center, Yale University, New Haven, CT 06520, USA

[d]Department of Pathology, Anatomy and Cell Biology, Meharry Medical College, Nashville, TN 37208, USA

Abstract

This study was performed to identify the potential role of Alpha-2 Heremans Schmid Glycoprotein (AHSG) in Head and Neck Squamous Cell Carcinoma (HNSCC) tumorigenesis using an HNSCC cell line model. HNSCC cell lines are unique among cancer cell lines, in that they produce endogenous AHSG and do not rely, solely, on AHSG derived from serum. To produce our model, we performed a stable transfection to down-regulate AHSG in the HNSCC cell line SQ20B, resulting in three SQ20B sublines, AH50 with 50% AHSG production, AH20 with 20% AHSG production and EV which is the empty vector control expressing wild-type levels of AHSG. Utilizing these sublines, we examined the effect of AHSG depletion on cellular adhesion, proliferation, migration and invasion in a serum-free environment. We demonstrated that sublines EV and AH50 adhered to plastic and laminin significantly faster than the AH20 cell line, supporting the previously reported role of exogenous AHSG in cell adhesion. As for proliferative potential, EV had the greatest amount of proliferation with AH50 proliferation significantly diminished. AH20 cells did not proliferate at all. Depletion of AHSG also diminished cellular migration and invasion. TGF-β was examined to determine whether levels of the TGF-β binding AHSG influenced the effect of TGF-β on cell signaling and proliferation. Whereas higher levels of AHSG blunted TGF-β influenced SMAD and ERK signaling, it did not clearly affect proliferation, suggesting that AHSG influences on adhesion, proliferation, invasion and migration are primarily due to its role in adhesion and cell spreading. The previously reported role of AHSG in potentiating metastasis via protecting MMP-9 from autolysis was also supported in this cell line based model system of endogenous AHSG production in HNSCC. Together, these data show that

*Corresponding author. Fax: + 1 615 327 6409. dmarshall@mmc.edu (D.R. Marshall)..

endogenously produced AHSG in an HNSCC cell line, promotes in vitro cellular properties identified as having a role in tumorigenesis.

Keywords

AHSG; HNSCC; TGF-β; MMP-9; Adhesion; Metastasis; Migration; Invasion

Introduction

Head and neck squamous cell carcinoma (HNSCC) includes cancers of the lips, oral cavity, salivary glands, nasal cavity, sinus, throat and larynx and is the 6th leading cause of cancer mortality in the world [1]. In 2012, it was estimated that approximately 37,000 Americans would be diagnosed with oral or pharyngeal cancer, with the preponderance diagnosed as late stages III and IV disease [2]. African-Americans are more likely diagnosed in advanced stages after adjustments for socioeconomic status, insurance status and other confounding factors [3]. The overall 5-year survival rate is 59%, although African-Americans have a 5-year survival rate of 39.5% which is broken down to 34% for African-American males and 52% for African American females [3, 4]. There are no prognostic markers or biomarkers for HNSCC and treatment is problematic due to a propensity for reoccurrence and loco-regional metastasis [5, 6]. Early diagnosis and an understanding of the progression of HNSCC would yield better results in treatment. In an attempt to identify serum biomarkers for HNSCC, we demonstrated that AHSG was elevated almost three times in the serum proteome of late stage HNSCC patients compared to controls and immunoblot analysis confirmed the presence of AHSG in primary tumors (Yarbrough and Marshall, unpublished data).

AHSG is a 63-kDa glycoprotein synthesized by the liver and secreted into the serum. The most widely accepted physiological function of AHSG is bone remodeling and inhibition of unwanted systemic ectopic calcification [7]. AHSG is associated with brain development and immune function including functioning as an anti-inflammatory mediator that participates in the inhibition of apoptosis of vascular smooth muscle cells [8]. It is a negative acute phase response protein [9], whose production decreases as disease load increases. We have shown, using *in vivo* animal models, that AHSG promotes breast cancer progression [9] and Lewis Lung Carcinoma tumorigenesis [10]. AHSG has been shown to be TGF-β receptor mimic in that its TRHI (TGF-β receptor II homology domain I) motif closely resembles the TGF-β receptor II in structure. Therefore the level of AHSG expression or secretion can significantly alter TGF-β signaling in tumor cells. For example in intestinal tumors where TGF-β drives tumorigenicity, more tumors were observed in AHSG (fetuin-A) knockout mice [9]. Lastly we demonstrated that AHSG is capable of stabilizing matrix metalloproteinases in solution and preventing their degradation by autolysis [11]. We therefore followed both TGF-β signaling and the expression of MMPs in these sublines of HNSCC and questioned whether these molecules altered the growth of the cells.

For decades, debate raged as to whether fetuin-A (the bovine homolog of AHSG) was the major adhesion protein in serum, particularly fetal bovine serum that is generally used to

supplement cell growth media *in vitro* [12]. We recently demonstrated using highly purified fetuin-A that it was the major attachment factor [13]. In the present study, we questioned whether AHSG, the human homolog of fetuin-A also supported attachment and growth of tumor cells. We also analyzed TGF-β signaling in the three sub-clones with different levels of AHSG expression.

In addition to these associations, AHSG has been shown to be a competitive inhibitor of TGF-β [11, 12, 14]. The TRHI motif in AHSG mimics TGF-β receptor II and therefore high expression and secretion of AHSG has the potential to down regulate TGF-β signaling. We therefore hypothesized that high expression of AHSG in EV and AH50 sublines would diminish TGF-β growth inhibitory properties but somehow reduce the growth of AH20 which express very low levels of AHSG.

Materials and methods

Materials

Polyclonal antibody to AHSG was purchased from Meridian (Cincinnati, OH, USA). Monoclonal antibodies to total SMAD, pSMAD 2/3, total Erk, pERK1/2 and GAPDH were purchased from Santa Cruz Biotechnology Inc., (Santa Cruz, CA, USA). Monoclonal antibodies to MMP-9, β-actin and α-tubulin were obtained from Cell Signaling (Danvers, MA, USA). Unless otherwise indicated, cell culture reagents were purchased from Invitrogen.

Cell lines

The HNSCC cell lines SQ20B, FaDu and UMSCC47 were kindly donated by Dr. Wendell Yarbrough (Yale University, New Haven, CT). SQ20B and FaDu were propagated in Dulbecco's modified Eagle's medium/nutrient F-12 (DMEM/F12), supplemented with 10% heat-inactivated fetal bovine serum (FBS)(Atlanta Biological), 250 μg/ml amphotericin B, 100 units/ml penicillin and 50 units/ml of streptomycin in a 95% air and 5% CO_2 incubator at 37 °C. DMEM/F12 without FBS or other growth factors is herein denoted serum-free medium (SFM).

Immunoblotting

Cells were grown in T-75 flasks to 80–90% confluence in CM or SFM as indicated. Cells were washed once in PBS (Invitrogen) and trypsinized with 2.5% trypsin (Invitrogen) and centrifuged at 5500 rpm for 7 min at 4 °C. Cells were lysed with RIPA buffer (50 mM Tris–HCl, pH7.4, 1% Nonidet P-40, 0.1% sodium deoxycholate, 150 mM NaCl, 1 mM EDTA) containing protease inhibitor mixture and phosphatase inhibitor (Sigma). Cell lysates were separated in 4–12% SDS-polyacrylamide gels (Invitrogen) and transferred to nitrocellulose membranes. Membranes were probed with 1:5000 of primary AHSG human anti-sheep polyclonal antibody (Meridian) and visualized by chemiluminescence (Bio-Rad). Densitometric quanitation of protein bands was performed using NIH Image J software.

Messenger RNA quantitation

Cells were cultured in T-75 flasks to 80–90% confluency in complete media. Cells were harvested by trypsinization, washed once in PBS and RNA was extracted using the Qiagen RNeasy kit (Valencia, CA). RNA measurements were obtained using a NanoDrop Spectrophotometer. The Qiagen One-step Platinum RT-PCR (VWR) kit was used to generate cDNA. The primers (Invitrogen, Carlsbad, CA) were AHSG sense (Fet1: 5′-GAGACTGTGACTTCCACATCC-3′) and AHSG antisense (Fet2: 5′-GGTTCCATTATTCTGTGTGTTG-3′). PCR reactions were performed in duplicate. The PCR of cDNA from the mRNA protocol was 50 °C for 50 min, 94 °C for 2 min, 94 °C for 30 s, 55 °C for 30 s, 68 °C for 1 min, and 72 °C for 7 min for 35 cycles. Real-Time PCR was accomplished with an IQ SYBR Green Supermix kit following the manufacturer's protocol (Bio-Rad). The copies of the targeted cDNA were normalized to α-tubulin.

RNAi

Viral stock for SQ20B transduction was generated by transfecting Phoenix cells (2×10^6 cells/well of a six well plate) with 6 μg/well of purified AHSG-targeted short hairpin RNA (shRNA) in plasmid pSM2c (Open Biosystems, Lafayette, CO). The sequences of the targeted sense region are AH50 5′ CGGTGCTCTTGCTAAGCTTA 3′ and AH20 5′ CGCTGTTGAAACTAGATGGCAA3′. The transfected Phoenix cells were cultured for 2–3 days, the supernatant was collected and virus was titered using Clontech Lenti-X™ GoStix™ (Mountain View, CA). SQ20B cells were transduced with 1 ml of $>5 \times 10^5$ IFU/ml of viral stock then cultured in DMEM-F12 CM with 5 μg/ml puromycin. Surviving clones were isolated and propagated in the same selection medium. Immunoblot analysis identified cells with diminished AHSG protein expression. The resulting cell lines were named as follows: SQ20B-EV (empty vector control), SQ20B-AHSG50 (knockdown expressing approximately 50% the amount of SQ20B-EV AHSG) and SQ20B-AHSG20 (expressing approximately 20% the amount of SQ20B AHSG).

Cellular proliferation assay

HNSCC cell lines SQ20B, FaDu and UMSCC47 and SQ20B transformed cell lines SQ20B-EV (EV), SQ20B-AHSG50 (AH50) and SQ20B-AHSG20 (AH20) were evaluated. Cells were plated, in triplicate, at 5×10^3 cells per well of a 24-well plate in SFM or CM with 1% Anti–Anti (Invitrogen). On days 0, 2, 4, 8, 10 and 12, media was removed and replaced with 100 μL of Presto-Blue diluted 1:10 in SFM. The cells were then incubated for 30 min at 37 °C. Proliferation, *via* cell viability was measured by fluorescence and is reported as arbitrary fluorescence units (AFU).

Cell attachment assay

Cell lines EV, AH50 and AH20 were used to assess the affect AHSG has on cellular adhesion. Cellular adhesion was assessed under two conditions: untreated wells with SFM and 30 μg/ml Laminin (Sigma) coated-wells. Prior to use in cell attachment assays, laminin coated plates were incubated for 40 min at 37 °C in 5% CO_2. Excess laminin was discarded and 2.2×10^4 cells in serum-free DMEM/F-12 were added to each well and incubated for 30 min at 37 °C. The cells were fixed in 4% Formalin (Fisher Scientific) and stained with

crystal violet. Adherent cells were counted by frame *via* 20× objective. Untreated plates were seeded and then incubated for 2 h at 37 °C. The cells were fixed in 4% Formalin, stained with crystal violet, and counted the same as above.

Migration and invasion assay

Transwell migration assay was performed using a BD migration chamber (BD Bioscience) with an 8 μm pore filter. Cell lines, EV, AH50 and AH20 were cultured in DMEM/F12 SFM for 4 days. 2×10^4 cells, in 400 μL of SFM, were loaded in the upper chamber and 600 μL of complete medium was added to the lower chamber. The plate was incubated at 37 °C for 24 h. Cell invasion was evaluated using BD Matrigel Invasion Chamber (BD Bioscience) with 8 μm pore polycarbonate filter with Matrigel™. The cells were loaded into the upper chamber at a density of 2×10^4/well in SFM and 600 μL of complete medium was added to the lower chamber. The plate was incubated at 37 °C for 24 h. Matrigel and/or cells on the insert membranes were removed using a cotton swab. Cells that had migrated through the insert membrane or invaded the Matrigel and insert membrane and reached the lower surface of the filter were subsequently fixed in 3% PFA in PBS, stained with crystal violet and counted using microscopy. Each experiment was performed in triplicate.

TGF-β signaling assays

Cell lines EV, AH50 and AH20 were cultured in SFM for three passages. Cells were then plated in 10 cm culture plates, in SFM for 24 h at 37 °C. The monolayers were washed in HBSS with 0.5mM Mg^{2+} and 0.5mM Ca^{2+} then treated with SFM supplemented with human recombinant TGF-β1 (Invitrogen) at 0, 10 or 100 ng/ml (in triplicate) and incubated for 15 min at 37 °C. Cells were then incubated, on ice, with ice cold PBS for 5 min then removed from the plate using a cell scraper, transferred to a 15 ml conical centrifuge tube and centrifuged at 5500 rpm for 5min. Cells were lysed with RIPA buffer containing a protease inhibitor P8340 (Sigma). 20 μg of cell lysates were separated in 4–12% SDS-polyacrylamide gels and transferred to nitrocellulose membranes. Membranes were probed with 1:1000 of primary pSMAD2/3 or 1:3000 total SMAD rabbit polyclonal antibody (Santa Cruz) or 1:1000 total Erk and 1:3000 pErk 1/2 (Santa Cruz), using chemiluminescence (Bio-Rad).

Zymography

MMP-9 activity was quantified by gelatin zymography of SF conditioned media and cell lysates from EV, AH50 and AH20. Non-reducing sample buffer (62.5mM Tris–HCl, pH 6.8; 10% glycerol; 0.1% bromophenol blue) was mixed with 8 μg of total protein from homogenate supernatants and electrophoresed on 9% SDS-polyacrylamide gels (SDS-PAGE) containing 0.1% gelatin (w/v). The gels were then washed (four times, 20 min each) at room temperature in 2.5% (v/v) Triton X-100 solution to remove excess SDS, transferred to zymogram development buffer, (Bio-Rad), and incubated for at least 18 h at 37 °C. Gels were fixed for 15 min with 50% methanol/7% acetic acid, washed for 30 min (six times, 5min each) with distilled water, stained for 1 h with Bio-Rad Colloidal Brilliant Blue G (Pierce, Rockford, IL), then rinsed with distilled water.

Statistical analysis

Statistical analysis was performed using GraphPad Prism 5. Each experiment was executed at least thrice. One-way ANOVA was used when there was only one variable to be considered and for multivariable analysis two-way ANOVA was used to statistically analyze data. In all cases a *p*-value <.05 is significant.

Results

AHSG expression in HNSCC cell lines

Initially we evaluated three human cell lines, SQ20B, FaDu and UMSCC47 for the presence of AHSG message and protein. Varying amounts of AHSG mRNA were detected, with SQ20B and FaDu showing greater expression than UMSCC47 (Fig. 1A and B). Immunoblot analysis confirmed the correlation between the AHSG message and protein (Fig. 1C). We hypothesized that AHSG enhances cell proliferation in AHSG-expressing HNSCC cell lines.

Fetal bovine serum (FBS), routinely used as a growth supplement for human cell lines, is a source of bovine AHSG. Therefore we used serum-free media (SFM) to evaluate endogenous AHSG production. We assessed whether the presence and abundance of AHSG significantly altered cellular proliferation and maintenance by quantitating SQ20B, FaDu and UMSCC47, plated in triplicate at 1×10^4 cells/well, over a period of 12 days. Cell numbers were determined using Presto Blue and fluorescent measurements were taken at 0, 4, 8 and 12 days, respectively. We observed that a decrease in cell numbers correlates to the amount of AHSG synthesized by each cell line (Fig. 1C and D). There were obvious decreases in proliferation that were noted at days 8 and 12 for both FaDu and UMSCC47 as compared to SQ20B. SQ20B cells reach a stationary phase of proliferation at day 8, while in comparison, FaDu and UMSCC47 reached their individual stationary phases of proliferation at day 4. By days 8 and 12, there were significantly fewer FaDu cells as compared to SQ20B and even fewer UMSCC47 cells (Fig. 1D) in culture. This is the first report of AHSG synthesis in human HNSCC cell lines and our data suggests that human AHSG functions as a growth factor *in vitro*. The SQ20B cell line, that produced the largest amount of AHSG, was selected for further analysis to investigate the correlation between endogenous AHSG levels and *in vitro* properties associated with metastasis.

Depletion of AHSG expression in the SQ20B HNSCC cell line

AHSG was targeted using five different AHSG-pGIPZ constructs. Two SQ20B clones were identified that expressed AHSG at levels approximately 50% (AH50) and 20% (AH20) of wild-type quantities (Fig. 2A and B). The AHSG sequences targeted for each of these clones are 5′ CGGTGCTCTTGCTAAGCTTA 3′ (AH50) and 5′ CGCTGTTGAAACTAGATGGCAA3′ (AH20). These two cell lines and an empty vector (EV) transfected cell line serving as a control, were evaluated to identify the influence of endogenous AHSG levels on adhesion, proliferation, migration, invasion and MMP-9 protection as well as the influence on TGF-β induced signaling *via* SMAD and ERK.

Cell proliferation and adhesion

EV, AH50 and AH20 were used to evaluate cell proliferation in the absence of exogenous AHSG. Viable cells were quantitated at days 0, 2, 4, 8 and 10. (Fig. 3A). Proliferation was greatly affected by the amount of endogenous AHSG produced by the SQ20B cell lines. From day 0 to 2, all cells appeared to be in a stationary phase of proliferation. At day four, we began to see a significant decrease in AH20 cell numbers as compared to EV (*p*-value=0096). We also noted that AH50 and EV started to move out of a lag phase and the rate of proliferation began to vary among these two cell lines. While AH20 cells never proliferated, EV and AH50 cells continued to proliferate (*p*-value=.0212) and by day 8, the difference in proliferating cells between AH20 and EV was even more significant, *p*-value=.0149 (Fig. 3A). On day 10, AH50 began to show a significant decrease in proliferation as compared to EV, *p*-value=.0029. These data support the hypothesis that AHSG plays a major role in the *in vitro* proliferation and maintenance of HNSCC cell lines. As squamous cells need to adhere prior to proliferation, we further tested whether the difference in proliferation could possibly be a consequence of the role of AHSG in cellular adhesion.

Cellular adhesion was assessed on both plastic (as the proliferation experiments were performed on plastic) and using laminin coated wells as an *in vitro* representative of extracellular matrix (Fig. 3B and C). In the laminin coated wells, we observed that at 30 min, EV was the first cell line to show signs of attachment followed by AH50 and lastly, AH20. On untreated plastic, attachment was seen at ~2 h and progressed in the same order as for laminin-treated wells. Cells were visualized microscopically and two fields per well were counted. There was a significant difference in the number of attached cells when comparing EV to AH50 and EV to AH20; *p*-value=.0302 and .0017, respectively (Fig. 3B). Collectively, this data suggest that AHSG mediates enhanced cellular proliferation through adhesion.

Role of AHSG in cell migration and invasion

Previously, we demonstrated a correlation between AHSG abundance, cell proliferation, adhesion and long-term viability. In assessing migratory potential, AH50 showed a statistically significant decrease in migration as compared to EV. An even greater decrease in migration was observed in AH20 (Fig. 4A and B) relative to both EV and AH50. Invasion for both AHSG knockdown cell lines was decreased relative to EV with AH50 decreased by approximately 50% and AH20 by almost 85% (Fig. 4C and D). Although migration and invasion do not always correlate, in this model these metastatic properties of AH50 and AH20 were both decreased. This reinforces our hypothesis that AHSG supports both invasion and migration in HNSCC. The mechanism by which AHSG mediates migration and invasion is not completely understood and requires further investigation.

AHSG as a competitive inhibitor of TGF-β1

The TGF-β pathway, acting as a tumor suppressor, has been linked to the mechanisms for migration and invasion in HNSCC [14–16]. We hypothesize that AHSG abrogates the tumor suppressor activity of the TGF-β pathway.We tested our hypothesis by treating cell lines EV, AH50 and AH20 with human recombinant TGF-β1 for 15min at 0, 10 and 100 ng/ml. Activation of the TGF-β pathway *via* phosphorylation of SMAD 2/3 was evaluated by

immunoblot. Alternative downstream effects were detected by measuring ERK phosphorylation. There was a negative correlation between AHSG expression and SMAD2/3 phosphorylation (Fig. 5A). In EV, SMAD phosphorylation was significantly less than in AH50 and AH20 cell lines. This data illustrated an increase in pSMAD in a dose dependent manner relative to the knockdown of AHSG, most specifically AH20. Contrary to these findings, knocking down AHSG resulted in decreased phosphorylated of Erk in both AH50 and AH20 as compared to the empty vector (Fig. 5C). At 0 and 10 ng/ml TGF-β, pErk is significantly less in AH50 and AH20 relative to EV. This data illustrated an decrease in pERK in a dose dependent manner relative to the knockdown of AHSG (Fig. 5B and D). Although adding exogenous TGF-β results in partial abrogation of the ERK pathway, it did not influence proliferation of our HNSCC cell lines (data not shown).

AHSG protection of MMP9

It is reported that MMPs are upregulated in most HNSCC patients, in particular MMP-1, 2, 9 and 11 [11]. Here, we hypothesize that AHSG protects MMP-9 from autolytic degradation, resulting in enhanced invasive potential and that the less endogenous AHSG there is in a cell line, the greater the degradation of MMP9. AHSG has been shown as a stabilizer of MMP-9, which results in consistent exposure of the MMPs to the basement membrane, compromising the integrity of the basement membrane [17]. Here this protectant nature of AHSG to MMP-9 is evaluated.

Cells were cultured for two days then conditioned media was collected. A significantly larger amount of MMP-9 protein was detected by immunoblot and zymography confirmed greater activity in both the EV and AH50 conditioned media relative to AH20 (Fig. 6A and E). These findings confirm that human AHSG prevents autolytic degradation of activated MMP-9 *in vitro*, and has the potential to enhance metastasis, through this mechanism, in HNSCC.

Discussion

The present study demonstrates that a number of established HNSCC cell lines synthesize AHSG and depletion of AHSG significantly decreases proliferation, adhesion, migration and invasion *in vitro*. Our data suggest that AHSG plays a role in tumorigenic properties of HNSCC. The liver produces most of the AHSG that is present in blood, which then is incorporated into cells [9, 14, 18]. For the first time we report that HNSCC cell lines synthesize AHSG and some of these cell lines also secrete the glycoprotein, resulting in an AHSG enriched micro-environment. In our HNSCC model we asked whether AHSG played a role in the adhesion and proliferation of HNSCC [9, 14]. We therefore undertook a systematic study, following knockdown strategies to demonstrate how AHSG affects molecular determinants of tumor progression including proliferation, migration and invasion in our HNSCC model.

It has been repeatedly reported that AHSG and its bovine homolog, fetuin-A are major drivers of cell proliferation both *in vitro* and *in vivo* [12, 13]. Guillory et al. reported that a lack of murine AHSG, in a murine model for breast cancer, resulted in delayed growth of mammary tumors [9]. Here we have established that endogenous AHSG synthesized by

HNSCC cells supports not only their rapid adhesion but also proliferation under serum free conditions. The present studies are in agreement with our previous studies, where we demonstrated that highly purified bovine fetuin-A/AHSG mediates not only the adhesion, but also the growth, of breast tumor cells under serum free condition [13]. The mechanisms by which AHSG promote adhesion, motility and cell proliferation are complex and warrant further in depth studies [9–11, 13, 18–22]. The significance of the data presented herein, is the demonstration that AHSG is as important as bovine fetuin-A, in the promotion of adhesion and growth of tumor cells *in vitro*.

The ability of AHSG to influence the speed of adhesion of HNSCC suggests that the protein also modulates focal adhesion assembly. Consequently the growth related signaling mechanisms that emanate from them such as those driven by focal adhesion kinase [10, 13], PI3 kinase/Akt and MAP kinases [9, 13]. Ultimately these pathways drive proliferation as we have shown for the bovine fetuin-A [9, 10, 13].

Previous studies suggested that AHSG plays a role in wound healing and motility in keratinocytes [23, 24]. Wang et al. reported that AHSG causes a significant morphological change in keratinocytes in cells exhibiting characteristics of migratory phenotype and cytoplasmic projections [24]. The mechanism in this work was not defined however they did report that the AHSG-associated migration activity of primary keratinocytes is largely independent of EGFR signaling and did not involve AKT1 or CDC42. However, Faber et al. found that SDF-1α had great effect on migration in CD44þCXCR4þHNSCC cell lines [25, 26]. We recently showed that purified fetuin-A was a powerful chemo-attractant for breast and colon cancer cells. HNSCC is frequently diagnosed with loco-regional metastasis [5, 27] and in fact, it is often referred to as a disease characterized by an occult, or unknown, primary due to the frequent presentation with an enlarged metastatic lymph node and no obvious primary lesion [5, 6, 28]. This suggests that some HNSCC cells are particularly adept at metastasizing before the primary tumor is even detected. It is possible that the ability to migrate within the confines of the tumor microenvironment may be facilitated by AHSG.

We previously demonstrated that AHSG interacts with MMPs, particularly MMP-9 and protects them from autolysis [11]. This is supported by this current data showing stable MMP-9 protein and associated enzymatic activities cells transfected with empty vector, and exhibiting 100% of wild-type AHSG protein levels, while MMP-9 protein and activity level is reduced in AHSG depleted cells. Interestingly, increased MMP-9 activity in HNSCC tumors has been reported [29–33]. This increase may be due in part to the increase of MMP-9 expression that is mediated by TGF-β1 [34].We show more MMP-9 activity in AH50 than EV. This may be due to the ability of TGF-β1 to enhance expression of MMP-9. The ability of AHSG to stabilize these enzymatic proteins could explain enhanced invasive capacity of the SQ20B (EV) and reduced invasiveness in the SQ20B-AHSG depleted cell lines AH50 and AH20.

Whereas the present data do not suggest that TGF-β plays an active *in vitro* role in adhesion, growth, motility or invasion of HNSCC, we cannot rule out its involvement *in vivo*. Increased expression of AHSG as HNSCC progresses is likely to neutralize TGF-β signaling

which has been shown to be inhibitory during transformation but is stimulatory in progressed and metastatic tumors [35].

In summary, the present work shows for the first time that AHSG is synthesized in human, non-hepatic cell lines and is a promoter of cell growth in head and neck squamous carcinoma cells specifically. We have also demonstrated that apart from growth promotion, AHSG promotes the motility and invasion of the tumor cells, suggesting that it is a molecular determinant of progression in HNSCC. The HNSCC cells that synthesize and secrete AHSG are therefore a valuable resource for studies aimed at understanding tumor progression and treatment modalities in head and neck cancers.

Conclusion

In conclusion, our data show multifaceted functions of AHSG in the progression of HNSCC. By depleting AHSG in the SQ20B cell line, we show decreases in adhesion, proliferation, migration and invasion. In future studies, transcriptomic and proteomic analyses of the depleted AHSG cell lines will be helpful in elucidating some of the effects associated with AHSG. This AHSG involvement with HNSCC may provide better insight into possible targets for therapeutic treatment.

Acknowledgments

This work was supported by grants from the SC1 CA134018-01 (JO); DOD W81XWH-07-1-0254 (JO); and U54 CA091408 (subproject DM) and 5 T32 HL007735-15 (SA). MMC Morphology Core is supported in part by NIH Grants U54MD007593, U54CA091408, G12MD007586, and S10RR0254970.

We thank Brandee Brown (VU), Joan Smith (MMC), and Kurt Watson (MMC) for their assistance with the production of this data.

REFERENCES

1. Vigneswaran N, Wu J, Song A, Annapragada A, Zacharias W. Hypoxia-induced autophagic response is associated with aggressive phenotype and elevated incidence of metastasis in orthotopic immunocompetent murine models of head and neck squamous cell carcinomas (HNSCC). Exp. Mol. Pathol. 2011; 90:215–225. [PubMed: 21236253]
2. Wang Y, Raj M, McGuff HS, Bhave G, Yang B, Shen T, Zhang X. Portable oral cancer detection using a miniature confocal imaging probe with a large field of view. J. Micromech. Microeng. 2012; 22
3. Ragin CC, Langevin SM, Marzouk M, Grandis J, Taioli E. Determinants of head and neck cancer survival by race. Head Neck. 2011; 33:1092–1098. [PubMed: 20967872]
4. Molina MA, Cheung MC, Perez EA, Byrne MM, Franceschi D, Moffat FL, Livingstone AS, Goodwin WJ, Gutierrez JC, Koniaris LG. African American and poor patients have a dramatically worse prognosis for head and neck cancer: an examination of 20,915 patients. Cancer. 2008; 113:2797–2806. [PubMed: 18839393]
5. Forastiere A, Koch W, Trotti A, Sidransky D. Head and neck cancer. N. Engl. J. Med. 2001; 345:1890–1900. [PubMed: 11756581]
6. Ridge JA, Lango MN, Feigenberg S. Head and neck tumors. Cancer Manage. 2011; 14
7. Osawa M, Umetsu K, Ohki T, Nagasawa T, Suzuki T, Takeichi S. Molecular evidence for human alpha 2-HS glycoprotein (AHSG) polymorphism. Hum. Genet. 1997; 99:18–21. [PubMed: 9003486]
8. Osawa M, Umetsu K, Sato M, Ohki T, Yukawa N, Suzuki T, Takeichi S. Structure of the gene encoding human alpha 2-HS glycoprotein (AHSG). Gene. 1997; 196:121–125. [PubMed: 9322749]

9. Guillory B, Sakwe AM, Saria M, Thompson P, Adhiambo C, Koumangoye R, Ballard B, Binhazim A, Cone C, Jahanen-Dechent W, Ochieng J. Lack of fetuin-A (alpha2-HS-glycoprotein) reduces mammary tumor incidence and prolongs tumor latency via the transforming growth factor-beta signaling pathway in a mouse model of breast cancer. Am. J. Pathol. 2010; 177:2635–2644. [PubMed: 20847285]
10. Kundranda MN, Henderson M, Carter KJ, Gorden L, Binhazim A, Ray S, Baptiste T, Shokrani M, Leite-Browning ML, Jahnen-Dechent W, Matrisian LM, Ochieng J. The serum glycoprotein fetuin-A promotes Lewis lung carcinoma tumorigenesis via adhesive-dependent and adhesive-independent mechanisms. Cancer Res. 2005; 65:499–506. [PubMed: 15695392]
11. Ray S, Lukyanov P, Ochieng J. Members of the cystatin superfamily interact with MMP-9 and protect it from autolytic degradation without affecting its gelatinolytic activities. Biochim. Biophys. Acta. 2003; 1652:91–102. [PubMed: 14644044]
12. Demetriou M, Binkert C, Sukhu B, Tenenbaum HC, Dennis JW. Fetuin/alpha2-HS glycoprotein is a transforming growth factor-beta type II receptor mimic and cytokine antagonist. J. Biol. Chem. 1996; 271:12755–12761. [PubMed: 8662721]
13. Sakwe AM, Koumangoye R, Goodwin SJ, Ochieng J. Fetuin-A ({alpha}2HS-glycoprotein) is a major serum adhesive protein that mediates growth signaling in breast tumor cells. J. Biol. Chem. 2010; 285:41827–41835. [PubMed: 20956534]
14. Swallow CJ, Partridge EA, Macmillan JC, Tajirian T, DiGuglielmo GM, Hay K, Szweras M, Jahnen-Dechent W, Wrana JL, Redston M, Gallinger S, Dennis JW. alpha2HS-glycoprotein, an antagonist of transforming growth factor beta in vivo, inhibits intestinal tumor progression. Cancer Res. 2004; 64:6402–6409. [PubMed: 15374947]
15. Derynck R, Akhurst RJ, Balmain A. TGF-β signaling in tumor suppression and cancer progression. Nat. Genet. 2001; 29:117–129. [PubMed: 11586292]
16. White RA, Malkoski SP, Wang XJ. TGFbeta signaling in head and neck squamous cell carcinoma. Oncogene. 2010; 29:5437–5446. [PubMed: 20676130]
17. Rosenthal EL, Matrisian LM. Matrix metalloproteases in head and neck cancer. Head Neck. 2006; 28:639–648. [PubMed: 16470875]
18. Leite-Browning ML, McCawley LJ, Jahnen-Dechent W, King Jr. LE, Matrisian LM, Ochieng J. Alpha 2-HS glycoprotein (fetuin-A) modulates murine skin tumorigenesis. Int. J. Oncol. 2004; 25:319–324. [PubMed: 15254728]
19. Kundranda MN, Ray S, Saria M, Friedman D, Matrisian LM, Lukyanov P, Ochieng J. Annexins expressed on the cell surface serve as receptors for adhesion to immobilized fetuin-A. Biochim. Biophys. Acta. 2004:111–123. (1693). [PubMed: 15313013]
20. Ochieng J, Pratap S, Khatua AK, Sakwe AM. Anchorage-independent growth of breast carcinoma cells is mediated by serum exosomes. Exp. Cell. Res. 2009; 315:1875–1888. [PubMed: 19327352]
21. Watson K, Koumangoye R, Thompson P, Sakwe AM, Patel T, Pratap S, Ochieng J. Fetuin-A triggers the secretion of a novel set of exosomes in detached tumor cells that mediate their adhesion and spreading. FEBS Lett. 2012; 586:3458–3463. [PubMed: 22980907]
22. Zhu WQ, Ochieng J. Rapid release of intracellular galectin-3 from breast carcinoma cells by fetuin. Cancer Res. 2001; 61:1869–1873. [PubMed: 11280740]
23. Wang XQ, Hayes MT, Kempf M, Fraser JF, Liu PY, Cuttle L, Friend LR, Rothnagel JA, Saunders NA, Kimble RM. Fetuin-A: a major fetal serum protein that promotes “wound closure” and scarless healing. J. Invest. Dermatol. 2008; 128:753–757. [PubMed: 17960182]
24. Wang XQ, Hung BS, Kempf M, Liu PY, Dalley AJ, Saunders NA, Kimble RM. Fetuin-A promotes primary keratinocyte migration: independent of epidermal growth factor receptor signalling. Exp. Dermatol. 2010; 19:e289–e292. [PubMed: 19758338]
25. Faber A, Goessler UR, Hoermann K, Schultz JD, Umbreit C, Stern-Straeter J. SDF-1-CXCR4 axis: Cell trafficking in the cancer stem cell niche of head and neck squamous cell carcinoma. Oncol. Rep. 2013; 29:2325–2331. [PubMed: 23563306]
26. Faber A, Hoermann K, Stern-Straeter J, Schultz DJ, Goessler UR. Functional effects of SDF-1alpha on a CD44(þ) CXCR4 (þ) squamous cell carcinoma cell line as a model for interactions in the cancer stem cell niche. Oncol. Rep. 2013; 29:579–584. [PubMed: 23232503]

27. Lin CJ, Grandis JR, Carey TE, Gollin SM, Whiteside TL, Koch WM, Ferris RL, Lai SY. Head and neck squamous cell carcinoma cell lines: established models and rationale for selection. Head Neck. 2007; 29:163–188. [PubMed: 17312569]

28. Strobel K, Haerle SK, Stoeckli SJ, Schrank M, Soyka JD, Veit-Haibach P, Hany TF. Head and neck squamous cell carcinoma (HNSCC)—detection of synchronous primaries with (18)FFDG-PET/CT. Eur. J. Nucl. Med. Mol. Imaging. 2009; 36:919–927. [PubMed: 19205699]

29. Erdem NF, Carlson ER, Gerard DA, Ichiki AT. Characterization of 3 oral squamous cell carcinoma cell lines with different invasion and/or metastatic potentials. J. Oral Maxillofac. Surg. 2007; 65:1725–1733. [PubMed: 17719389]

30. Kaomongkolgit R. Alpha-mangostin suppresses MMP-2 and MMP-9 expression in head and neck squamous carcinoma cells. Odontology/Soc. Nippon Dent. Univ. 2012

31. Ondruschka C, Buhtz P, Motsch C, Freigang B, Schneider-Stock R, Roessner A, Boltze C. Prognostic value of MMP-2, -9 and TIMP-1, -2 immunoreactive protein at the invasive front in advanced head and neck squamous cell carcinomas. Pathol. Res. Pract. 2002; 198:509–515. [PubMed: 12389993]

32. Roy R, Yang J, Moses MA. Matrix metalloproteinases as novel biomarkers and potential therapeutic targets in human cancer. J. Clin. Oncol.: Off. J. Am. Soc. Clin. Oncol. 2009; 27:5287–5297.

33. Schmalfeldt B, Prechtel D, Harting K, Spathe K, Rutke S, Konik E, Fridman R, Berger U, Schmitt M, Kuhn W, Lengyel E. Increased expression of matrix metalloproteinases (MMP)-2, MMP-9, and the urokinase-type plasminogen activator is associated with progression from benign to advanced ovarian cancer. Clin. Cancer Res.: Off. J. Am. Assoc. Cancer Res. 2001; 7:2396–2404.

34. Sinpitaksakul SN, Pimkhaokham A, Sanchavanakit N, Pavasant P. TGF-beta1 induced MMP-9 expression in HNSCC cell lines via Smad/MLCK pathway. Biochem. Biophys. Res. Commun. 2008; 371:713–718. [PubMed: 18457660]

35. Freudlsperger C, Bian Y, Contag Wise S, Burnett J, Coupar J, Yang X, Chen Z, Van Waes C. TGF-beta and NF-kappaB signal pathway cross-talk is mediated through TAK1 and SMAD7 in a subset of head and neck cancers. Oncogene. 2013; 32:1549–1559. [PubMed: 22641218]

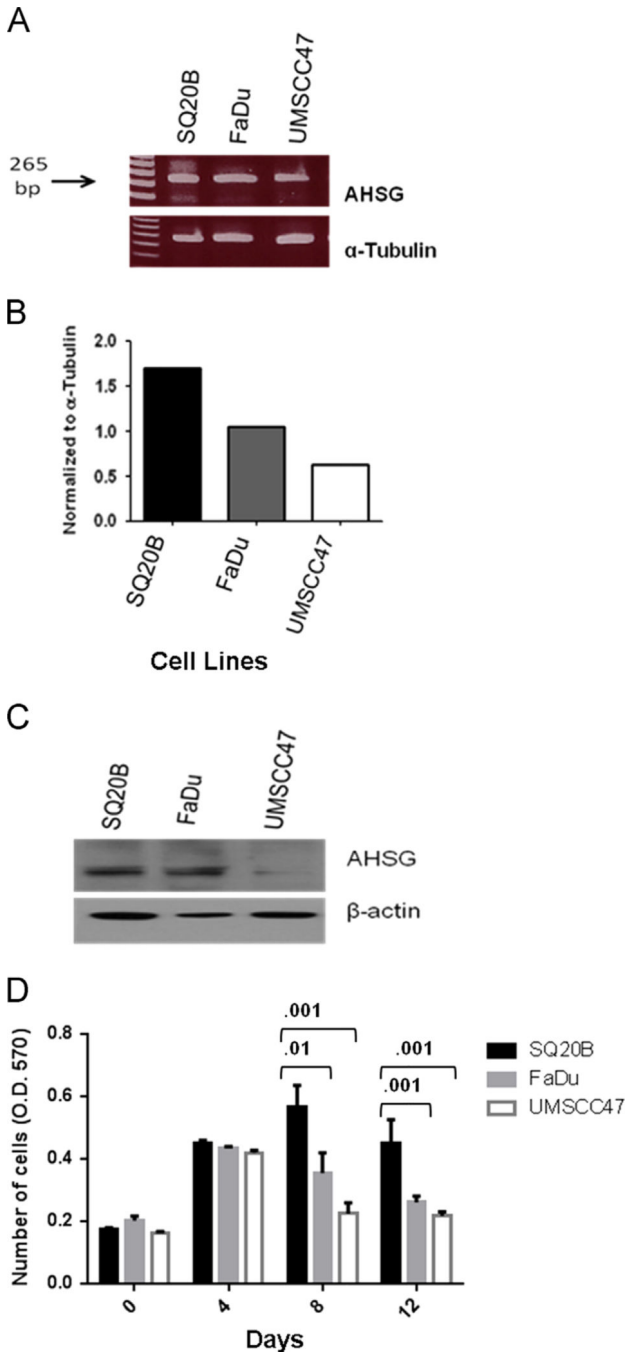

Fig. 1.

AHSG message and protein levels in HNSCC cell lines. (A) HNSCC cell lines FaDu, SQ20B and UMSCC47 were serum-starved for 48 h. Cells were washed twice with PBS. RNA was extracted using the Qiagen RNeasy Kit. Equal concentrations of each RNA sample were used to detect mRNA expression. (B) Densitometric analysis of AHSG and β-actin. AHSG relative expression was determined by normalization to β-actin. (C) The indicated HNSCC cell lines were serum-starved for 48 h. Cells were washed twice with PBS and cells were removed from the flask by scraping to ensure intact cell surface receptors

were included. Protein was released from cells in RIPA buffer. Equal amounts of proteins were dissociated and analyzed in 4–12% SDS gels and immunoblotting with the indicated antibodies. (D) Cells were harvested by trypsinization, rinsed and SQ20B, FaDu and UMSCC47 were resuspended in serum-free medium. Cells (1×10^4 cells/well) were seeded in SFM in 24-well plates, and incubated at 37 °C. A total of 4 plates per experiment were seeded and at days 0, 4, 8 and 12, Presto Blue was added at a ratio of 1:10 and absorbance read at 570 nm after incubation for 30 min at 37 °C to give relative viable cell numbers. Bars represent mean cell numbers ± SD from three independent experiments.

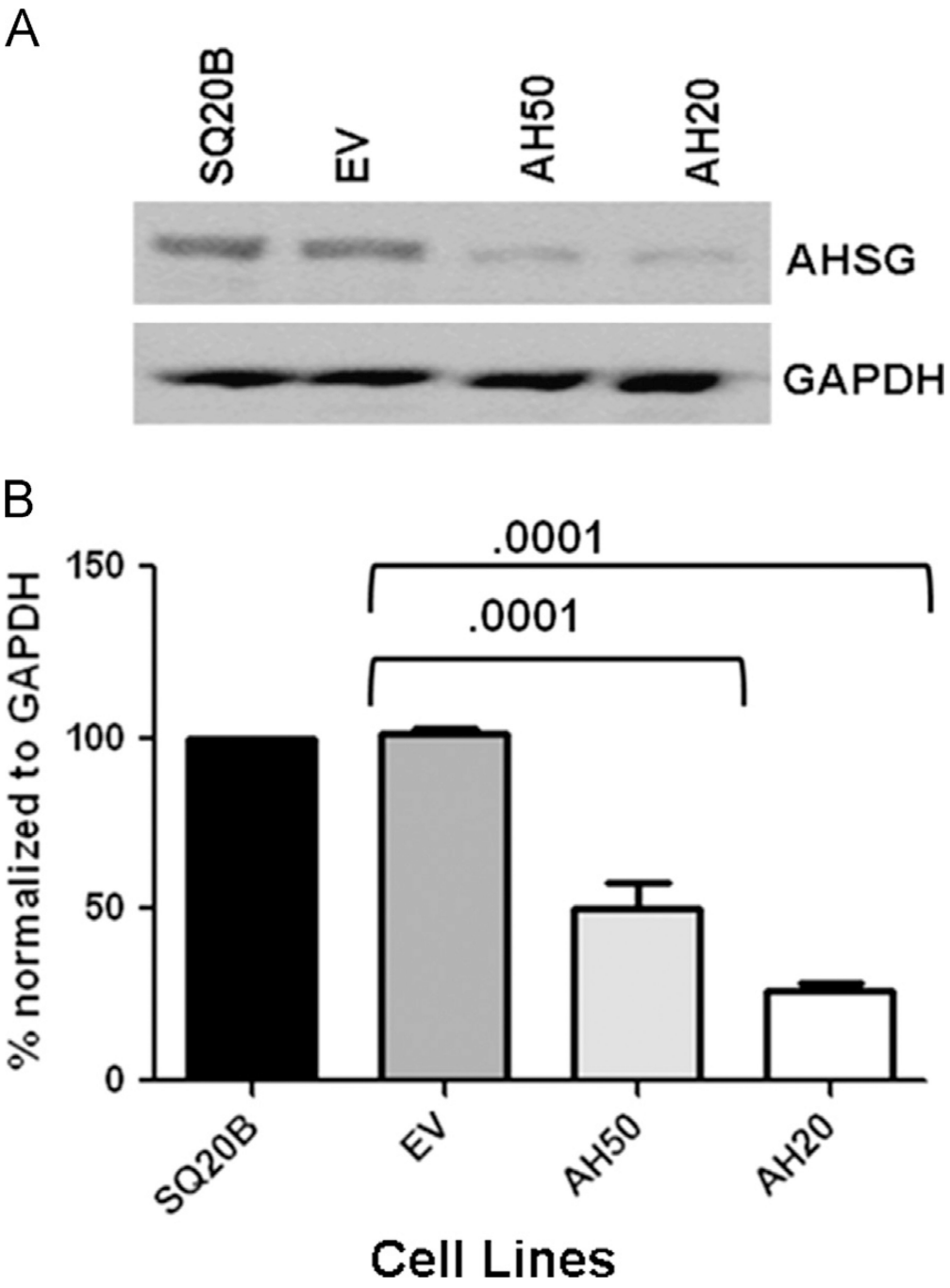

Fig. 2.

RNAi Mediated AHSG Subline Generation from the SQ20B HNSCC Cell Line. (A) Parental SQ20B cells were transduced with empty vector (EV) or small hairpin RNAs (AH50 and AH20) targeting distinct regions of the coding sequence of AHSG. Stable puromycin-selected clones were expanded and the extent of AHSG depletion assessed by immunoblotting using antibodies against AHSG. (B) Densitometric analysis of AHSG expression of AHSG-depleted SQ20B sublines. AHSG expression levels were normalized to

GAPDH. Bars represent AHSG expression ± SD from three independent experiments relative to the expression level in the parental SQ20B cells.

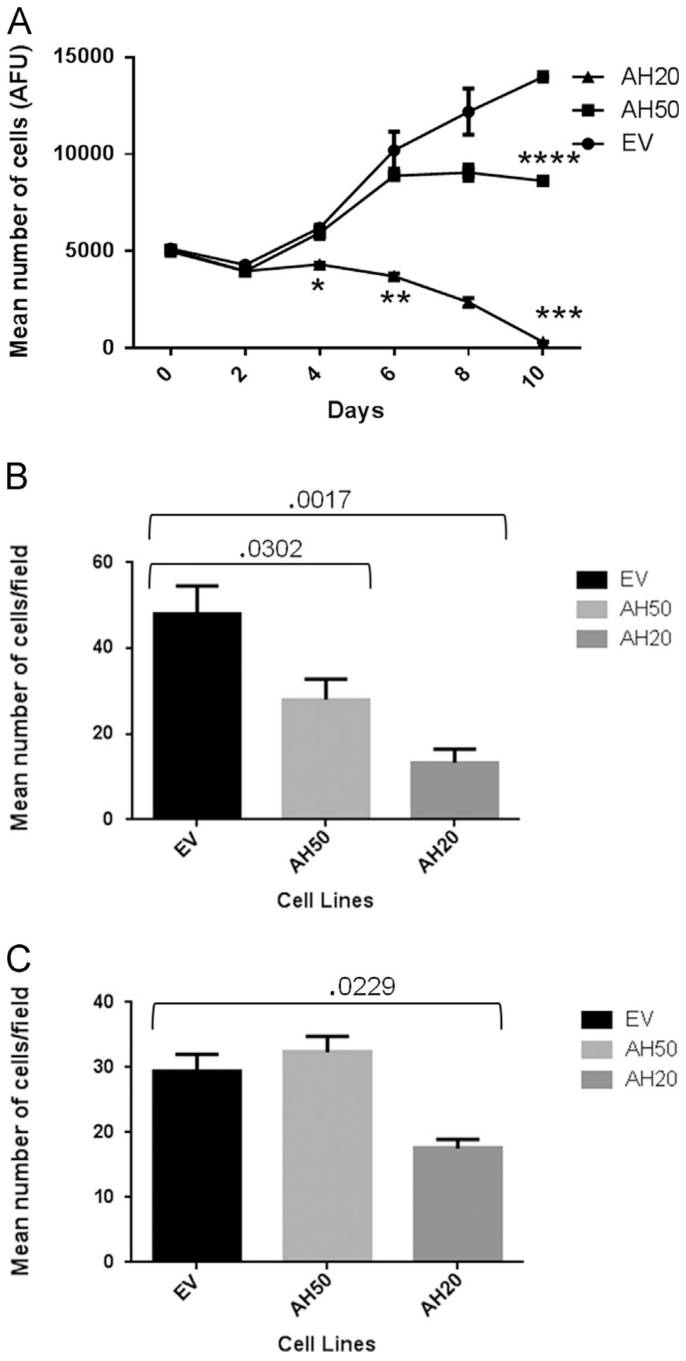

Fig. 3.

AHSG drives the adhesion and proliferation of human SQ20B HNSCC sublines EV, AH50 and AH20. (A) Cells were harvested by trypsinization, rinsed in SFM and EV, AH50 and AH20 were re-suspended in SFM (DMEM/F12). Cells (5×10^3 cells/well) were seeded in 24-well plates, and incubated at 37 °C. At day 0, 2, 4, 6, 8 and 10, Presto Blue was added at a ratio of 1:10 and the plates were read in fluorescence plate reader (Excitation 535 nm; Emission 590 nm) after 30min of incubation to give arbitrary fluorescence units (AFU) as a measure of relative numbers of viable cells (*p*-value * =.009, ** =.01, *** =.0003 and ****

=.003). GraphPad Prism was used for statistical analysis. (B) Sublines of SQ20B cells, EV, AH50 and AH20 were harvested using 2mm EDTA, rinsed and resuspended in SFM. Cells (2×10^4 cells/well) were seeded in laminin coated wells and incubated for 30 min at 37 °C. The cells were fixed in 4% Formalin and stained with crystal violet. Adherent cells were counted under a microscope (20× objective) and reported as relative number of cells/field of view. (C) The sublines EV, AH50 and AH20 were harvested as above (panel B) and same number of cells seeded in uncoated (plastic) wells and incubated for 2 h at 37 °C and relative number of adherent cells determined as in panel B.

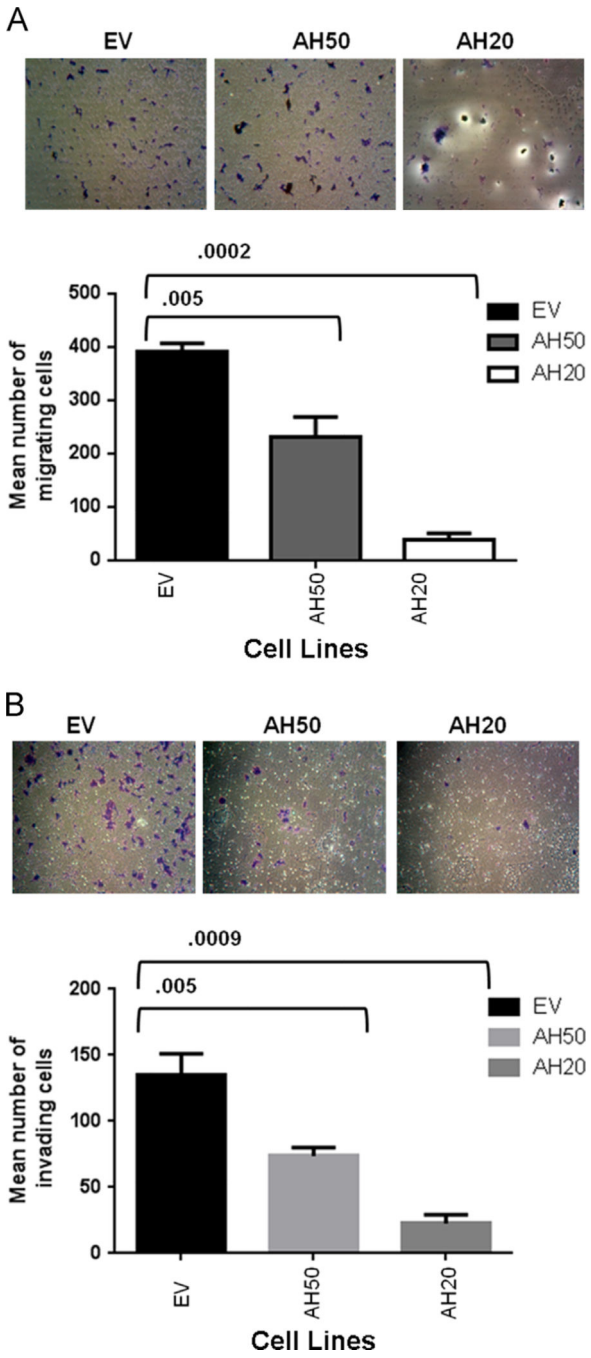

Fig. 4.

AHSG promotes the motility and invasion of human SQ20B HNSCC sublines EV, AH50 and AH20. A) Cells were harvested by trypsinization, washed abundantly in SFM and 2.5 × 10^4 cells plated in triplicate in the upper chambers of 8 μm culture inserts (panel A) or the inserts containing a thin layer of Matrigel (panel B) in 24 well plates. Complete DMEM/F12 was added to the lower chambers followed by incubation at 37 °C for 24h. After incubation, the media and floating cells in the upper insert chamber were aspirated and removed with a cotton swab and cells migrated to the underside of the filters fixed and stained with crystal

violet. Migrated cells were photographed and counted. Bars represent the mean number ± SD of migrated (panel A) or invading (panel B) cells/field of view.

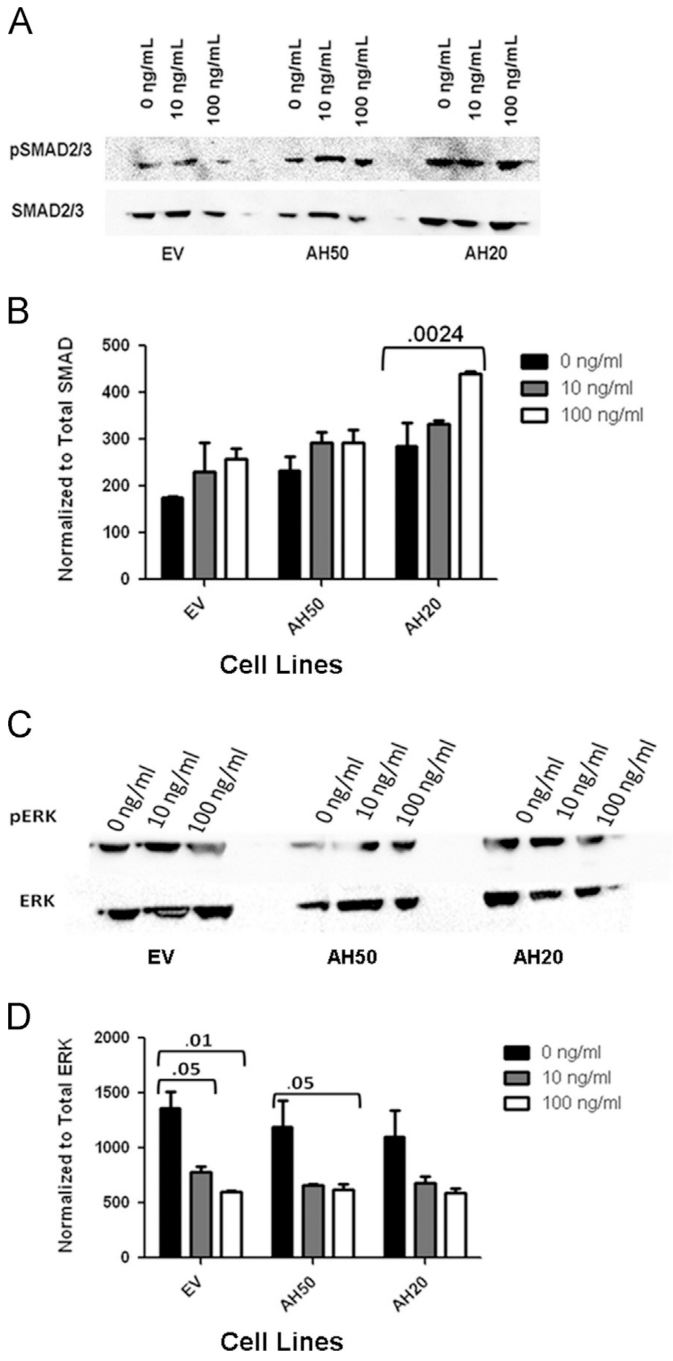

Fig. 5.

Effect of AHSG depletion on TGF-β1 induced signaling in human SQ20B HNSCC sublines EV, AH50 and AH20. (A–D) Sublines, EV, AH50 and AH20, were seeded and then serum-starved for 48 h. Sublines were treated with 0, 10 or 100 ng/ml of human recombinant TGF-β1 in HBSS for 15 min at 37°C. Total cell lysates were prepared and equal amounts of protein used for analyses by immunoblotting. (A) Phosphorylation of SMAD2/3 was examined by immunoblot using antibody to phosphorylated SMAD 2/3 and was compared to immunoblot of total SMAD 2/3. (B) Densitometric quanitation of the activation of

SMAD2/was performed following treatment with indicated TGF-β1. Phosphorylation of SMAD2/3 was normalized to total SMAD2/3. (C) The sublines EV, AH50 and AH20 were treated and harvested as above. Phosphorylation of ERK was examined by immunoblot using antibody to phosphorylated ERK; detection of total ERK was used for normalization. (D) Densitometric analysis was used to normalize pERK bands to total ERK.

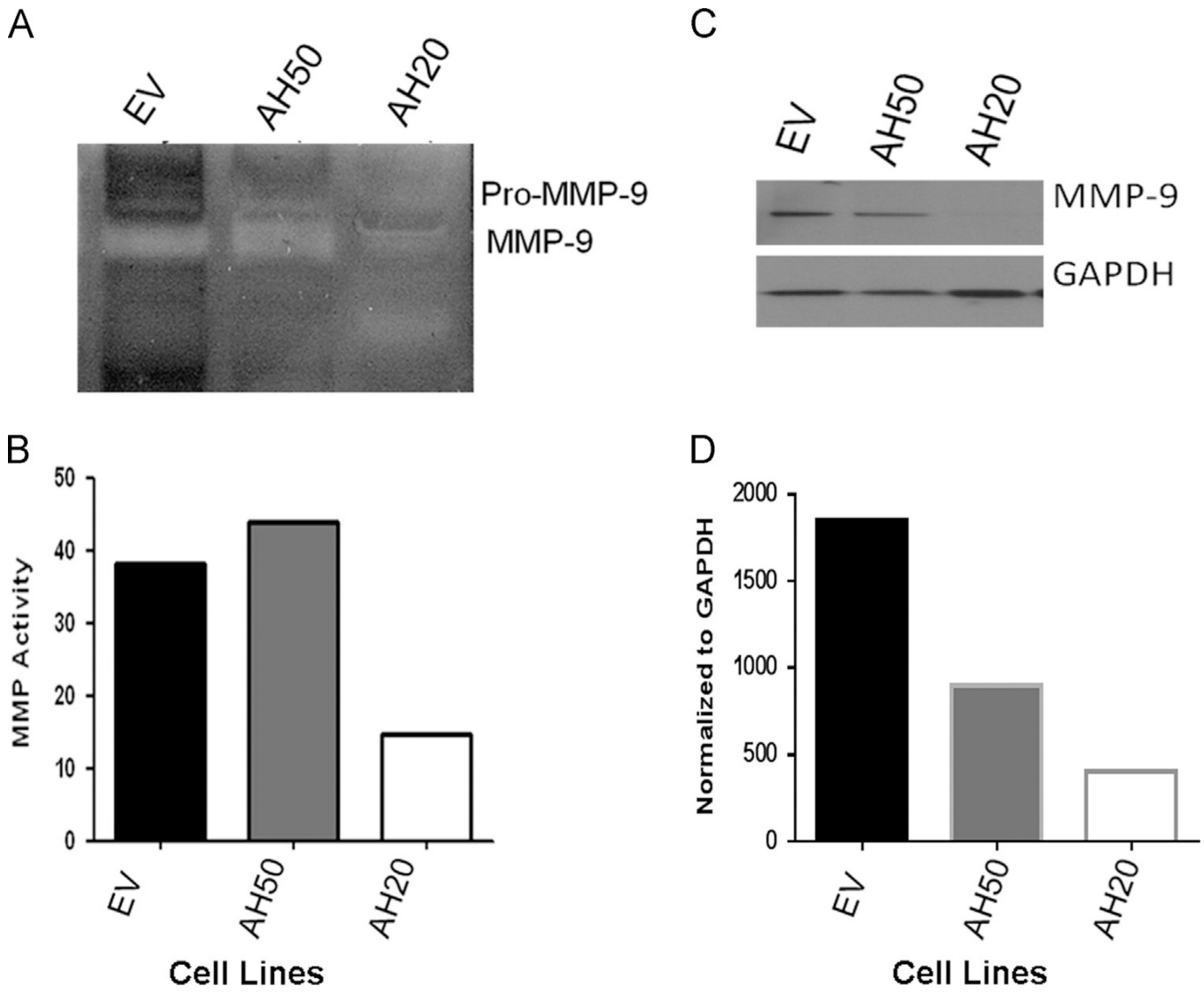

Fig. 6.

AHSG protects MMP-9 from autolytic degradation in SQ20B HNSCC sublines EV, AH50 and AH20. EV, AH50, and AH20 were cultured in serum-free media for 96 h. (A) Conditioned medium from each cell line was collected and 6 ml of each was used for ultrafiltration to a final volume of 100 μl. Equal concentrations were dissolved in zymography sample buffer and analyzed. Serum-free EV conditioned medium was used as the control. (B) Densitometric quantitation of the zymogram for MMP-9 in (A). (C) MMP- 9 protein in the concentrated conditioned medium from EV, AH50 and AH20 was quantitated by immunoblot using antibodies to MMP-9. MMP-9 bands were normalized to GAPDH and depicted in (D).